Eur Arch Psychiatry Clin Neurosci (1997) 247:61–70

ORIGINAL PAPER

Stefan Pauli · Göran Sedvall

Three-dimensional visualization and quantification of the benzodiazepine receptor population within a living human brain using PET and MRI

Received: 11 November 1996 / Accepted: 18 November 1996

Abstract Positron emission tomography (PET) in combination with receptor-selective high-affinity radioligands allows the characterization of neuroreceptor distributions in the living human brain. Thus far, the visualization and quantification of receptors with PET have been limited to series of two-dimensional (2D) image planes of the anatomic receptor distribution. The development of high-resolution PET has increased the number of planes to approximately 50, supplying an excessive amount of image information from a single experiment. The inherent limitations of 2D techniques make them insufficient to apprehend and efficiently analyze this cumbersome amount of data. In the present communication we describe procedures to visualize and quantify in three dimensions (3D) the total image information from the compound set of 47 2D planes of a PET experiment using commercially available software. Three-dimensional computer graphic and volume rendering techniques were used to analyze and display the results. For the experimental application the benzodiazepine (BZ) antagonist [^{11}C]flumazenil was used as radioligand to visualize the BZ receptor (BZR) population in the brain of a healthy human subject. Three-dimensional images of the radioligand binding receptor population were displayed with regard to volume and form in relation to the corresponding anatomic structures in the brain reconstructed from MR images. The volume-rendering technique allowed the inspection of PET signals representing BZR populations in the interior of the hemisphere as viewed from the medial projection. Thresholding and seeding techniques were used to define volumes and quantities. Using the PET data and volume rendering, the total amount of cerebral BZRs ($N_{Cerebrum}$) and the apparent volume they take into account ($V^{app}_{BZR,\ Cerebrum}$) could be calculated for the first time using an automated procedure. The cerebrum of the healthy subject contained 17.6 nmol of BZRs in a voulume of approximately 1.25 L. The principles and application of the technical development described offer new dimensions to clinical neuroscience and should be practically useful for automated quantitative determination of neuroreceptor number in brain regions of patients with neuropsychiatric disorders and in relation to drug treatment.

Key words Benzodiazepine receptors · Positron emission tomography · MRI · [^{11}C]Flumazenil · Human brain · Volume rendering · 3D Visualization · 3D Quantification

Introduction

The development of brain imaging techniques during the past two decades has allowed the exploration of blood flow and general metabolism in regions of the living human brain (Sokoloff et al. 1977; Latchaw et al. 1995). Such general functions in brain regions are now explored as to changes in relation to psychological and neuropsychiatric variables and categories in human subjects (Friston et al. 1991; Raichle 1994; Andreasen et al. 1995a, b; Fiez et al. 1996).

To gain deeper insight into biological functions mediating neuropsychiatric signs and symptoms, the detailed exploration of molecular neurotransmitter mechanisms in the human brain is required (Sedvall et al. 1986). Neurotransmitter receptors are essential components in such an analysis.

During the past two decades the development of selective radioligands with high affinity to neuroreceptors has allowed the visualization and quantification of anatomical neuroreceptor distributions in the animal and human brain during in vitro conditions (Kuhar et al. 1991; Hall et al. 1994). By using positron emission tomography (PET), radioligand binding to neuroreceptors can be directly recorded in the living brain of healthy subjects and in patients with neuropsychiatric disorders (Wagner et al. 1983;

S. Pauli (✉) · G. Sedvall
Department of Clinical Neuroscience, Psychiatry Section, Karolinska Institute and Hospital, S-171 76 Stockholm, Sweden,
Tel.: +46 8 729 54 20; Fax: +46 8 34 65 63;
e-mail: stefanp@psyk.ks.se

Farde et al. 1986). Such techniques are appropriate for producing the first comprehensive maps, atlases and data banks for human living brain biochemistry (Roland and Zilles 1994; Sedvall et al. 1986; Sedvall and Farde 1995).

In previous PET studies on neuroreceptors their gross in vivo distribution has been presented and measured in series of 2D planes. Quantification is usually obtained from manually drawn regions of interest (ROIs). The development of high-resolution PET technology (HRPET) has significantly increased the number of planes – presently approximately 50, supplying an excessive amount of information from a single PET experiment (Weinhard et al. 1994). To extract the information from such a compound set of 2D images into apprehensible meaningful quantitative information concerning neuroreceptor populations in defined volumes and structures new approaches are required. This is irrespective of whether the acquisition of radioactivity in the PET camera is made in 2D- or 3D mode. Thus, a major scientific problem consists of making this cumbersome 3D data matrix comprehensible and to develop practical methods for comparative clinical studies.

During the past 2–3 decades various techniques for 3D computer graphics have been developed (Toga 1990; Russ 1995). Among those it has recently become apparent that volume rendering has a number of advantages, e.g., the possibility to automatically visualize, delineate and quantify not only the surface but also the interior of objects. (Harris et al. 1978, Herman and Liv 1979; Drebin et al. 1988). The data can be registered by a diversity of medical instruments such as laser scanning confocal microscopes, PET and magnetic resonance (MRI) scanners. However, the technique of volume rendering has not previously been used in PET studies of neuroreceptors.

Gamma aminobutyric acid (GABA) is the most abundant inhibitory transmitter in the brain. Benzodiazepine receptors (BZRs) are important components of the $GABA_A$-receptor/chloride channel complex which is regulated by GABA. The quantitative distribution of BZRs in the human brain should accordingly reflect the GABA-receptor distribution and give aspects of the potential for inhibitory transmission in brain regions. Previously, the use of PET and the BZ antagonist [^{11}C]flumazenil to examine BZR binding in the human brain has been described (Mazière et al. 1984; Persson et al. 1985; Blomquist et al. 1990; Lassen 1992; Price 1993; Lammertsma et al. 1993; Lassen et al. 1995).

The aim of the present study was to use the compound set of 2D image planes obtained from a PET-scan experiment to spatially visualize BZR binding within the whole-brain volume of a living human subject, by applying 3D computer graphic technique and volume rendering. We used this approach to develop an efficient practical method to quantify the total BZR number in the whole brain and in defined volumes. The total receptor number, rather than the receptor concentration, represents an alternative dimension of a global transmitter function in a human individual that has not previously been focused upon in neuropsychiatric research. Such a measure may turn out to give useful information for exploratory neuropsychiatric research (Sedvall et al. 1994).

Methods

The measurements were performed on a 29-year-old man. He was healthy according to physical examination and routine blood and urine analyses.

To obtain a similar positioning of the brain in the MRI and PET investigations a plastic helmet was prepared to fixate the head in the cameras (Bergström et al. 1981).

Image acquisition

MRI data

The subject was investigated by MRI prior to the PET experiment. Using a MR Signa Advantage System (Signa 1.5 T, General Electric, Milwaukee, Wis., USA) scanner at the Karolinska Hospital (Sweden), a fast 3D gradient-echo pulse sequence (FSPGR) was used which gave a full coverage of the entire brain with 124 contiguous slices with a thickness of 1.5 mm and no gap between the planes. In the axial plane the resolution was 1.5 mm and the quadratic field of view (FOV) of each plane had a side of 260 mm and was represented by 256 × 256 pixels. The corresponding voxel size was 1 × 1 × 1.5 mm in the x, y, and z dimension.

A box with copper sulfate in plastic tubes was used to create position landmarks (cf. Bergström et al. 1981). Visual inspection of the MRI images did not disclose any abnormalities in the brain of the healthy volunteer. The MR images were transferred from the MRI scanner to a Silicon Graphics computer (Onyx, RealityEngine^2, Silicon Graphics Inc., Mountain View, Calif.) to be stored on the hard disk (Fig. 1).

PET data

The PET study was performed using a Siemens ECAT Exact HR 47 (Siemens, Erlangen, Germany) at the Karolinska Hospital. In the camera there are 24 rings, each with 784 detectors. After image reconstruction, 47 planes with 3.125 mm interplanar distance were acquired covering an axial distance of 15 cm (Weinhard et al. 1994). Each plane was made up of 128 × 128 square pixels with a side 2.0 mm. The corresponding voxel size was 2.0 × 2.0 × 3.125 mm in the x, y, and z dimensions. The in-plane resolution of the images reconstructed was approximately 3.7 mm full width at half maximum (FWHM).

The radioligand [^{11}C]flumazenil was synthesized as previously described (Halldin et al. 1988) When the subject had been positioned in the PET camera, a cannula was inserted in the left antecubital vein. Approximately 350 MBq [^{11}C]flumazenil of high-specific radioactivity (> 1000 Ci/mmol) was injected intravenously. Immediately after the injection, the cannula was flushed with 10 ml of saline.

After injection of the radioligand, PET scanning was performed during 63 min in 22 contiguous time intervals (frames) during which data was collected. Because the time activity curve changes rapidly at the beginning of the experiment, the first frames were given a shorter duration (30 s) than the later ones (6 min.). The frames corresponding to the time interval from 12 to 63 min were summed and used for further analysis in the present study. In this way the summation image will represent the presence of the radioligand in the brain at a time when the ligand distribution phase has ended, i.e., after approximately 9 min (Persson et al. 1989).

During the last frame a box was inserted around the subject's head in the field of view of the PET camera. The box had plastic tubes filled with a low amount of radioactivity in order to create position landmarks (Bergström et al. 1981). As mentioned previ-

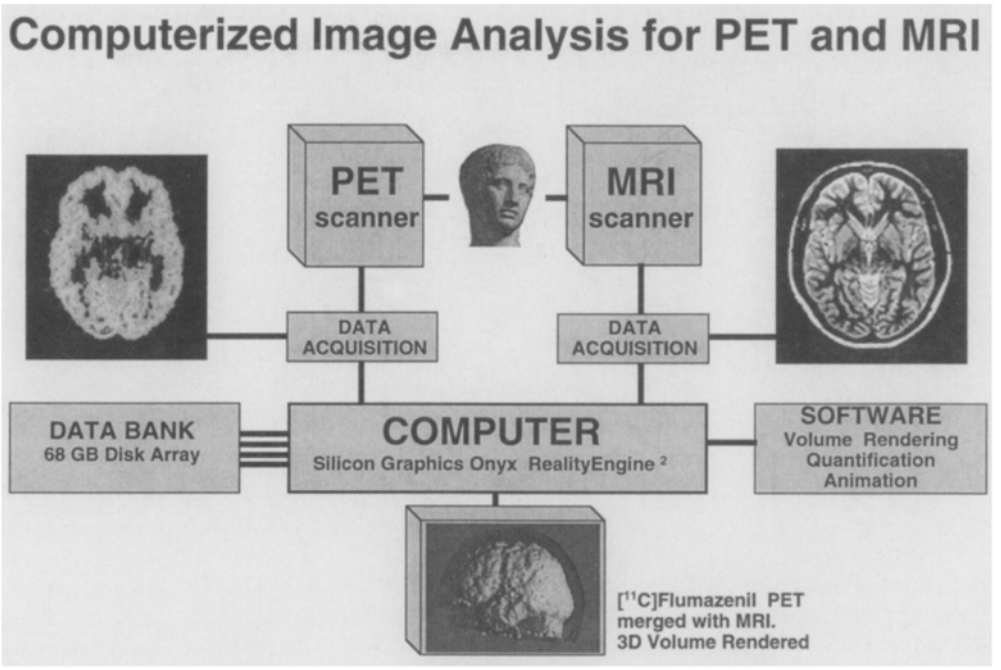

Fig. 1 Outline of data acquisition and image analysis for positron emission tomography (PET) and magnetic resonance imaging (MRI)

ously a similar box with copper sulfate landmarks was used during the MRI run. By means of these landmarks the PET and MRI images could subsequently be aligned (see below).

Because the PET experiment did not include the complete extension of the cerebellum, the subsequent quantitative determinations were based on data where the part of cerebellum recorded by PET was excluded.

Image preprocessing

The original MRI and PET data were transferred to the Silicon Graphics computer system (Silicon Graphics, Inc., Calif., USA) (Fig. 1). Here the different image formats were converted to the same format, and for both MRI and PET the voxels were made cubic in shape, the same size and equal in number. This was achieved by using interpolation among the data points recorded to resample the pixels in the PET planes to the same size as the MRI pixels (1 mm). Because in PET and MRI the interplanar distance is larger than the in-plane pixel side, additional planes were created by interpolation to make the new interplanar distance equal to the original pixel side, thereby creating voxels that are cubic in shape. In this study an algorithm was used which allows a precise specified distance between the new interpolated planes equal to the x–y pixel side. After this preprocessing, the PET and MRI voxel matrices each had $256 \times 256 \times 150$ equally large cubic 1-mm voxels. All these interpolations were made using the program VoxelMath 2.2 (Vital Images, Inc., Fairfield, Iowa, USA).

To simultaneously visualize the PET and MRI voxel matrices in a merged mode they had to be aligned. The registration of the two modalities was performed by overlaying image plans from the PET and MRI voxel matrices and then translating and rotating them under manual control in relation to each other until the landmarks from the boxes in PET and MRI coincided. The MRI voxel matrix was tilted by 7° forward in the sagittal plane, and displaced 4 mm in the positive z-direction to achieve this goal. These transformations were also made using the program VoxelMath.

Volume rendering

Medical imaging instruments primarily present scalar data in two dimensions: S(x,y). The 2D techniques for visualization and quantification of structures in images have been the dominating paradigm for the analysis of scientific data. Many areas demand more than 2D surface mapping of an object to be correctly interpreted and understood, e.g., the interior of a body.

In the late 1970s the first attempts were made to describe the interior of the human body by volume rendering, based mainly on X-ray tomographic data (Harris et al. 1978; Herman et al. 1979). The landmark computer graphic technique to perform volume rendering was developed by Pixar Inc. (USA) and described in a pioneering paper by Drebin et al. (1988).

There are two kinds of 3D rendering: *surface rendering* or as it is currently termed, "shaded surface display" (SSD) and *volume rendering*. In surface rendering mathematical algorithms create surfaces from the scalar data in the voxel matrix (Lorenson and Harvey 1987). Artificial surfaces are thereby constructed which implicitly introduce discontinuities in the data. In volume rendering (Drebin et al. 1988; Wilhelms et al. 1991) this problem is avoided by employing a technique that directly presents the data within a voxel and uses all voxels in the voxel matrix.

Voxel data

The voxel information from PET (radioactivity concentration) and MRI (hydrogen density) is arranged in a number of parallel planes (Fig. 2). Each picture element (pixel) in the plane is a sample of the parameter recorded. It corresponds to a certain volume element (voxel) which can be thought of as a small box with the pixel as bottom and the interplanar distance as height. These voxels make up a 3D matrix which is converted to an isotropic 3D grid with cubic voxels as described previously by using interpolation techniques. The voxels have to be cubic in shape in order to maintain correct proportions of the rendered image independent of rotation angle under which the voxel matrix is viewed.

Volume rendering techniques

The basic concept in volume rendering is that each data point, radioactivity for PET and hydrogen amount for MRI, is mapped into a single voxel, and that each voxel is projected into one or more pixels onto an image screen in order to visualize the voxel matrix from different angles (Fig. 2). Each voxel is assigned a color in terms of red, green and blue, and partial opacity, which are both related to the value (radioactivity or hydrogen amount) of the corresponding data point. Each pixel on the image screen is given a color determined by blending of color and opacity of all the voxels

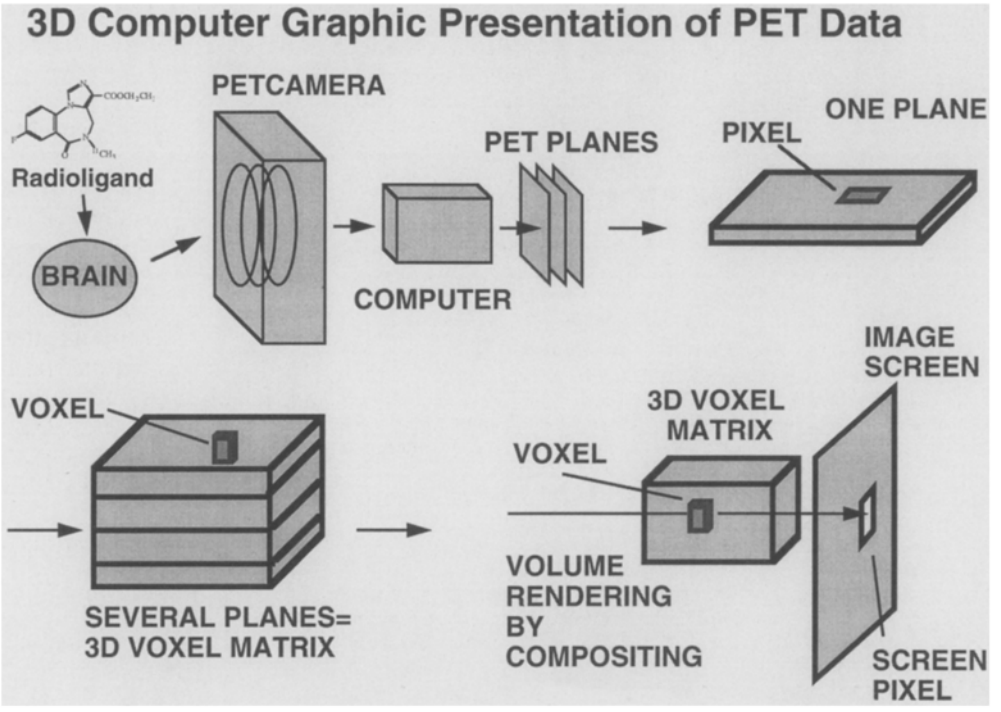

Fig. 2 Principles for 3D computer-graphic presentation of PET data using volume rendering

that are on a line of sight perpendicular to the image screen and passing through the above-mentioned pixel.

In the present study the compositing or back-to-front-projection method was used (Catmull 1974; Watt 1991; Russ 1995). In this approach for volume rendering the calculation starts at the distal (in relation to the image screen) part of the voxel matrix and rays are cast from the voxels to the pixels of the image screen. This method is faster and less memory demanding than other methods such as the ray-tracing method (Levoy 1988). The compositing method may use bi- or trilinear interpolation to sample among neighboring voxels along the path of the ray. The projection is drawn from back to front which makes it possible for the viewer to dynamically observe the reconstruction of the object, layer by layer, until the final image is completed.

By assigning a high opacity to high and medium radioactivity voxels from the PET data, it is possible to selectively visualize BZRs in the neocortex with its sulci and gyri where the voxels have a high radioactivity using [^{11}C]flumazenil as in the present study. On the other hand, high uptake areas can be made relatively less visible by making lower uptake areas more visible giving the possibility to visualize structures behind the surface. This is achieved by adjusting the opacity to emphasize or de-emphasize the high- and low-uptake voxels accordingly.

To further enhance the impression of a varied surface, a lighting model according to Phong (Foley et al. 1990) can be added. Light is cast on the surface which reflects light (highlights) and also gives rise to shading. The compositing rendering technique is implemented in the computer program VoxelView/Ultra 2.2 (Vital Images, Inc., Fairfield, Iowa, USA) which was used in this work.

Merging modalities

The PET and MRI voxel matrices merged together can be visualized simultaneously or alternatively (see Fig. 6). The PET voxel matrix can be emphasized or de-emphasized in relation to the MRI matrix. These manipulations were also made by the program VoxelMath. For example, the PET data could be emphasized to replace the MRI data where they exist simultaneously. By using different color scales for the MRI data (blue scale) and/or the PET data (Sokoloff scale) the two image modalities could be distinguished in the same image. This discrimination made it possible to visualize the relative position of the BZR population (PET) in the brain in relation to the anatomy of the skull and the brain (MRI).

Quantification of BZR binding

The radioactivity concentration designated to the voxel matrix from the PET experiment with [^{11}C]flumazenil represents radioligand specifically bound to BZR (B) in addition to free (F) and nonspecifically bound radioligand. Previous PET and autoradiographic experiments indicate that radioactivity in the pons region, with insignificant BZR density, reflects predominantly free radioligand concentration (Persson et al. 1989; Blomqvist et al. 1990; Hall et al. 1992). Thus, radioactivity in the pons was used as a measure of free radioligand concentration in the brain (F) based on the assumption that nonspecifically bound radioligand was insignificant.

The radioactivity concentration within the pons was determined in the following way. Manual drawing of the pons ROI (region of interest) was made in all the MRI planes covering the extension of the pons (nos. 10–35 counted from the bottom of the voxel matrix). These regions were extracted as a pons voxel volume V_{pons} and transferred to the PET voxel matrix using the program VoxelMath and a boolean function. The pons volume was calculated by multiplying the number of voxels in the V_{pons} by the volume of each voxel. The radioactivity concentration in pons (F) was calculated by dividing the total radioactivity content of V_{pons} given by the volume radioactivity integral of the pons by its volume.

To calculate the BZR amount in the cerebrum, data for the cerebellum were excluded from the PET voxel matrix. Data for the cerebellum were removed as follows: Cerebellum was delineated on all the MRI planes covering the extension of this region (MRI planes 1–58). The corresponding cerebellar volume was removed from the PET matrix giving a matrix for the cerebrum exclusively. Because the midbrain and parts of the brainstem included contain minute amounts of BZRs in relation to the cerebrum, the part of the PET matrix excluding the cerebellum should represent predominantly the cerebrum. To exclude radioactivity artefacts from the outside of the brain and from white matter (WM) inside the brain, the PET matrix for cerebrum was thresholded at a level corresponding to the highest WM value. This was done in the following way. Using MR slice nos. 81–87, i.e. above the ventricles, the WM volume included in these slices was extracted using a thresh-

old for the MR signal by the program VoxelMath. This WM volume was transferred to the PET voxel matrix. To remove spill-over effects from cortical radioactivity, this WM volume was reduced by *erosion* (4 pixel layers, Russ 1995). The highest PET voxel radioactivity value within this eroded VM matrix was used as the threshold level for the PET matrix. The volume of voxels above this value was grown by adding three voxel layers using *dilation* (Russ 1995) to incorporate all voxels between the highest WM value and the free radioligand concentration F, 170 nCi/cc. In this way an apparent volume representing voxels for specific binding, $V^{app}_{BZR,\ Cerebrum}$, was obtained. The average cerebral radioactivity was calculated by dividing the radioactivity volume integral of cerebrum by its volume.

A second approach, the *seeding method* was used to determine the apparent BZR volume. This implies that a *seed voxel*, i.e., a PET voxel with a certain *seed value*, was chosen within the PET cerebrum matrix. The *seed value* was set equal to F. All voxels with higher radioactivity than the *seed value*, and which have a direct or indirect physical contact with the *seed voxel*, are included in the seeded volume by this seeding procedure.

According to the Michaeli–Menten equation the following relation holds true:

$$B = B_{max} \cdot F / (F + K_d) \quad (1)$$

where: B = concentration of radioligand bound to receptors "bound"; B_{max} = receptor concentration (Hall et al. 1992); F = free radioligand concentration ("free"); and K_d = equilibrium dissociation constant.

When high specific radioactivity of the ligand is used, as in the present study, F is small in relation to K_d. Thus, when a small amount of free radioligand (F) is present in the brain, Eq. (1) can thus be rewritten as:

$$B_{max} = (B/F) \cdot K_d \quad (2)$$

$$B = T\text{-}F, \quad (3)$$

where B is calculated as the average total radioligand concentration (T) minus the average free (F) radioligand concentration. The value used for K_d, 8.6 nmol, was obtained from previous PET experiments with varying specific radioactivities of [^{11}C]flumazenil (Persson et al. 1989).

The total receptor number $N_{Cerebrum}$ was calculated using values measured according to Eq. (4):

$$N_{Cerebrum} = V^{app}_{BZR,\ Cerebrum} \cdot K_d \cdot (T\text{-}F) / F, \quad (4)$$

where $N_{Cerebrum}$ = total receptor number (nanomoles) and $V^{app}_{BZR,\ Cerebrum}$ = cerebral BZR containing volume.

Results

In Fig. 3 the consecutive 47 PET planes covering most of the brain in the healthy subject are visualized using the Sokoloff (1977) color-coding procedure. As shown before, neocortical, cerebellar and limbic cortices showed a high accumulation of radioactivity after [^{11}C]flumazenil injection. Because a high specific radioactivity and a low mass of the radioligand was used in the PET experiment, the radioactivity levels showed in the 47 images reflect the density of BZRs (see Eq. (1)). Note that the lower part of the cerebellum was not covered by the PET planes. Therefore, the cerebellum was deleted in the quantitative measures.

In Fig. 4 the surface of the voxel matrix containing radioactivity from the PET experiment is visualized from six different angles. In this way a 3D visual impression of the topography of the BZ population in the brain of the healthy volunteer was obtained. Although the PET resolution is fairly low, it is apparent from Fig. 4 that the 3D volume-rendering technique could be used to depict the gyral topography of the BZRs in the neocortex of the human brain.

To visualize BZR populations within the hemisphere as observed from an interior view, the PET voxel matrix was transsectioned in the medial sagittal plane and the left half was deleted. Figure 5 illustrates the remaining half of the voxel matrix representing the right hemisphere. This part of the voxel matrix was rotated around a vertical axis using the animation part of the program VoxelView. In Fig. 5 the three top illustrations visualize the exterior surface of the voxel matrix. In the two lower rows of illustrations the interior of the hemisphere is visualized from different angles. Because the basal ganglia have a relatively low density of BZRs, these receptor populations became less visible with the opacity setting used. This procedure accordingly allowed a presentation of the BZR-rich parts of the interior aspect of the neocortex. Thus, in the middle row and also in Fig. 6 the BZRs of the interior side of the neocortex and in the insular cortex are visualized from an interior view. In this case the PET voxel matrix was merged with the MRI voxel matrix, which allows the visualization of the PET data for receptor binding with their correct anatomical context at the same time.

Figure 7 presents an oblique view from below the exterior surface of the seeded volume of the PET data representing BZR binding. The deleted part of the cerebellum data is visualized in red. To the right some of the corresponding 2D PET planes are presented. The intersection of the white lines indicate the point where the seeding process was initiated.

The volume of the pons, V_{pons}, was found to be 7490 mm^3. The value for free radioactivity concentration in pons (F) was 170 nCi/cc. Using the *threshold method* the BZR containing volume, $V^{app}_{BZR,\ Cerebrum}$, was measured to 1.253 L. The *seeding method* gave a volume of 1.249 L. The total average radioactivity in the cerebrum (T "total") was 448 nCi/cc. By substituting the average of the two cerebral volume values obtained by the thresholding and seeding methods for $V^{app}_{BZR,\ Cerebrum}$ in Eq. (4), together with the numerical values for K_d, T, and F, the total cerebral BZR number, $N_{Cerebrum}$, was calculated to 17.6 nmol.

Discussion

The present single case study represents the first attempt to apply automated 3D computer graphic methods to present and quantify neuroreceptor binding data from a PET experiment. A combination of automated and manual computer graphic methods were described and used to visualize and quantify in 3D the BZR distribution in the brain of a healthy human subject.

Until recently, most efforts to visualize 3D information have utilized conventional geometric graphic technique. This involves the organization of the data to be presented into a model composed of geometric surface primitives

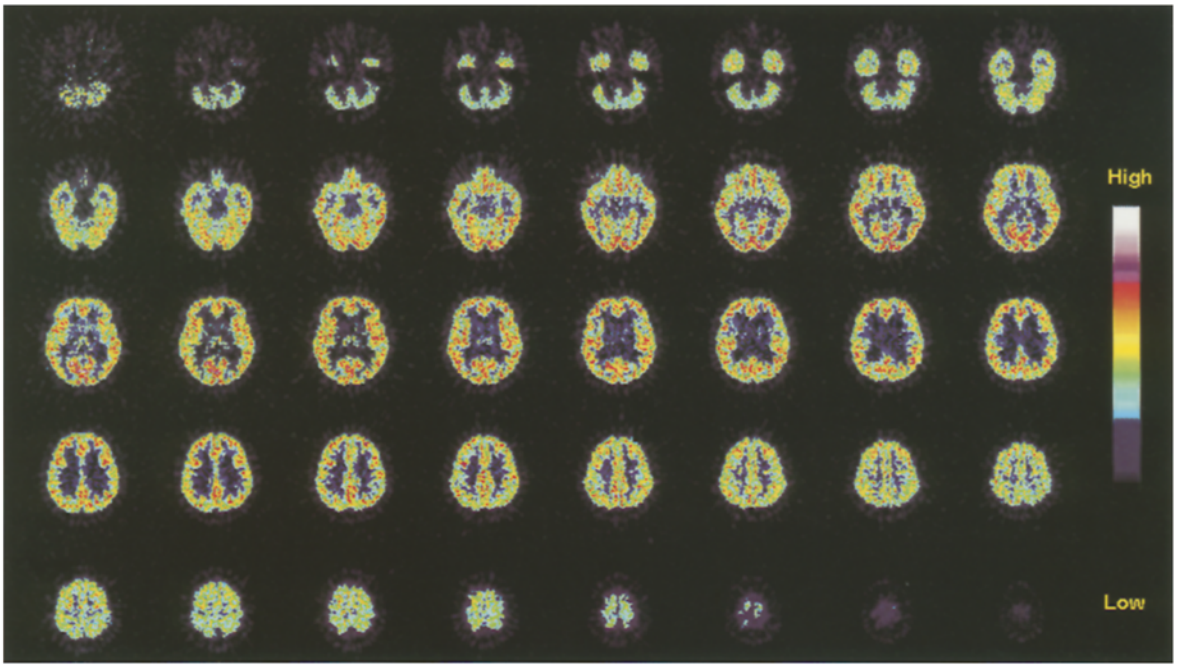

Fig. 3 Benzodiazepine receptor binding in the brain of a healthy volunteer. [^{11}C]Flumazenil binding is presented in 47 PET planes. The *color scale* indicates relationship between level of radioactivity and color. The *figures* represent radioactivity accumulation during 12–63 min after radioligand injection

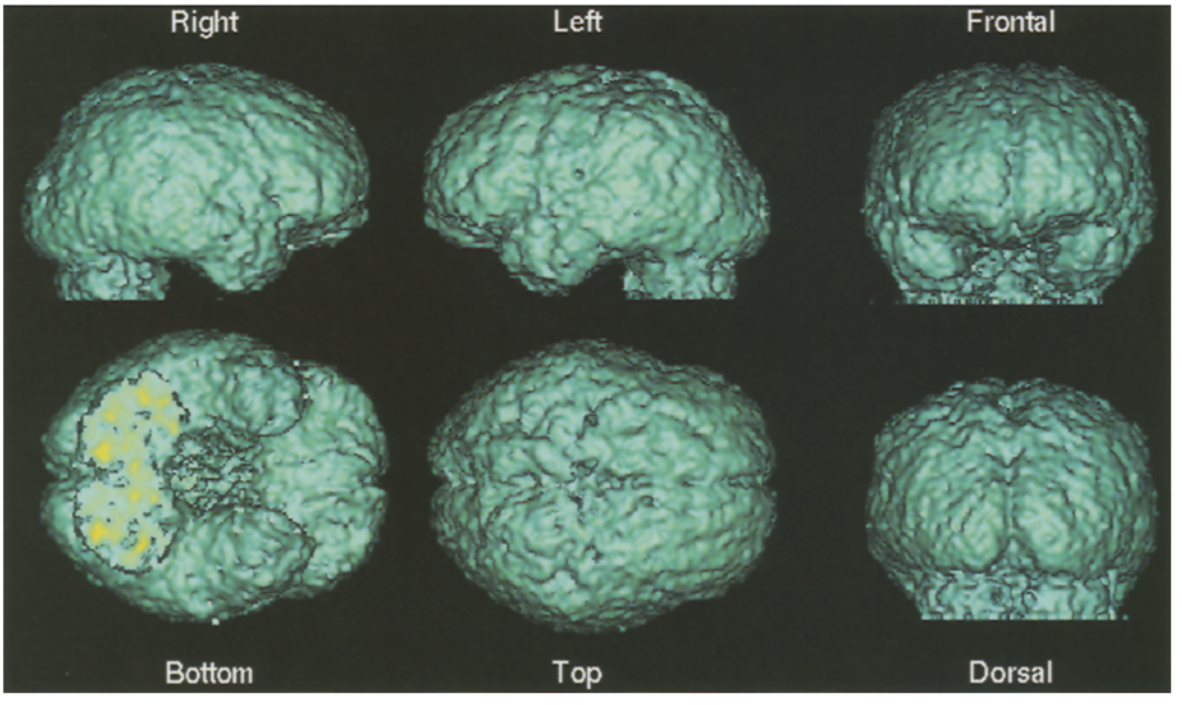

Fig. 4 A 3D volume rendering of PET data for benzodiazepine receptor binding in the brain of a healthy volunteer. PET and the benzodiazepine antagonist [^{11}C]flumazenil was used. The figures represent radioactivity accumulation during 12–63 min after radioligand injection

such as points, lines, or polygons (Van Zandt 1989; Argiro 1990). In the present study we selected volume rendering as a more efficient and practical 3D technique (Drebin et al. 1988). The BZ antagonist [^{11}C]flumazenil was used to record, present, and quantify radioligand-binding data from the whole voxel matrix obtained from a PET experiment in a healthy human subject.

The 3D rendering techniques use the same information as a set of 2D image presentations from a PET experiment. Thus, they do not contain any additional informa-

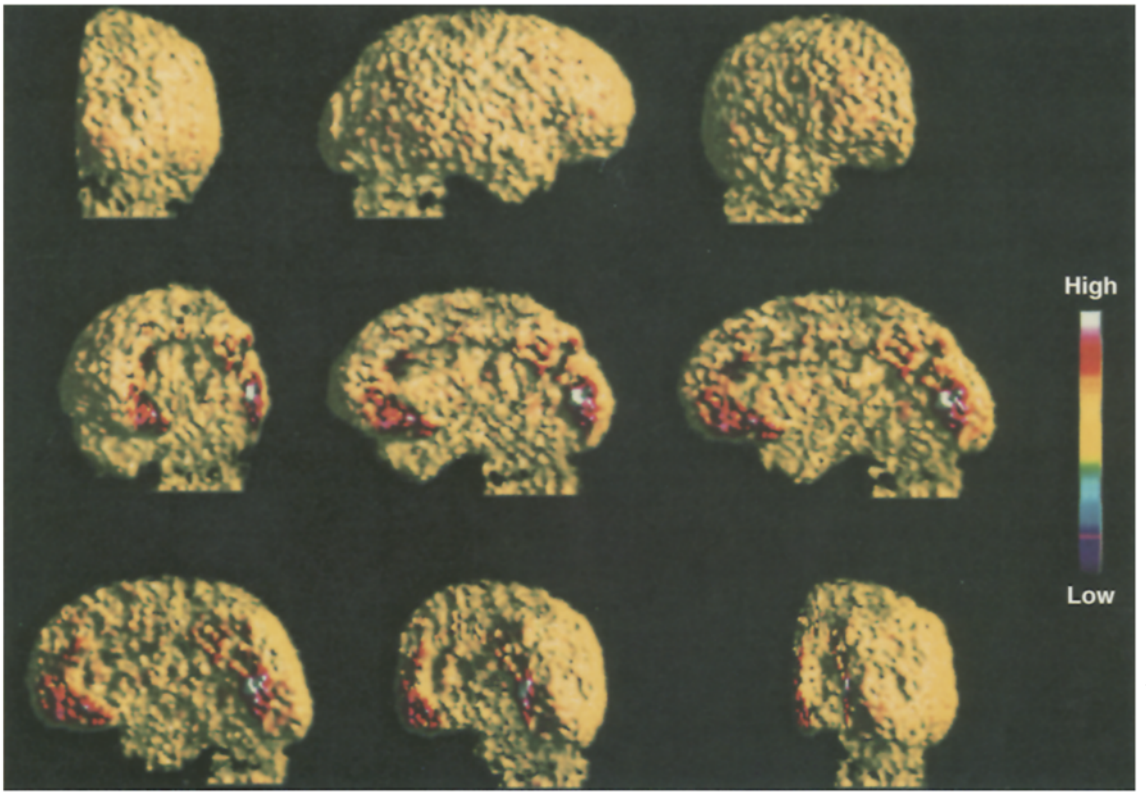

Fig. 5 A 3D volume rendering of benzodiazepine receptor binding as recorded by PET and [^{11}C]flumazenil in a healthy man. The 3D radioactivity voxel matrix for the left half of the brain was deleted. The remaining voxel matrix for the right brain half is successively rotated around a vertical axis in 10° increments in the nine panels. The *three top panels* show the exterior of the surface of the benzodiazepine receptor (BZR) population in the right half of the brain. The *lower panels* show the interior of the benzodiazepine containing neocortex including the insula in some projections

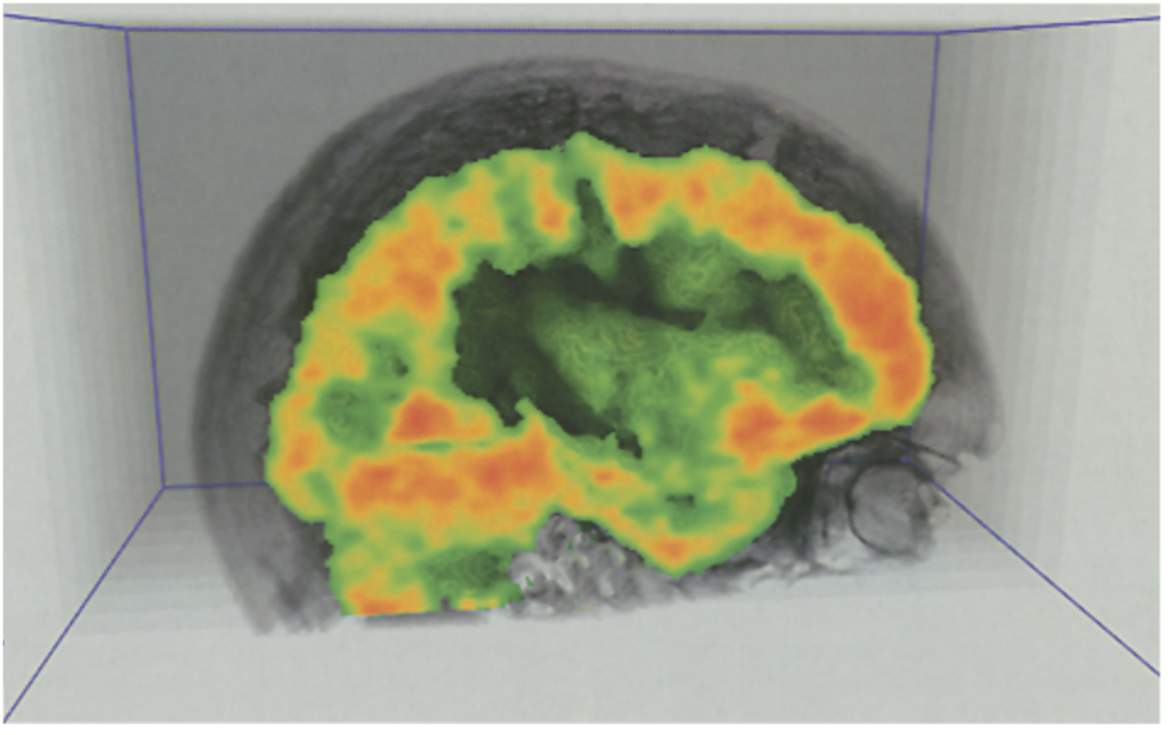

Fig. 6 This image represents a view from inside the left hemisphere cut along the parasagittal plane and is constructed from the PET and MRI voxel matrices. Note the clear visualization of the BZR population in the interior of the insular cortex as well as in the interior of the cortex below the central sulcus. The skull is the surrounding *dark structure* (MRI) and the brain (PET) is shown in a *red* (high)/*green* (low) scale

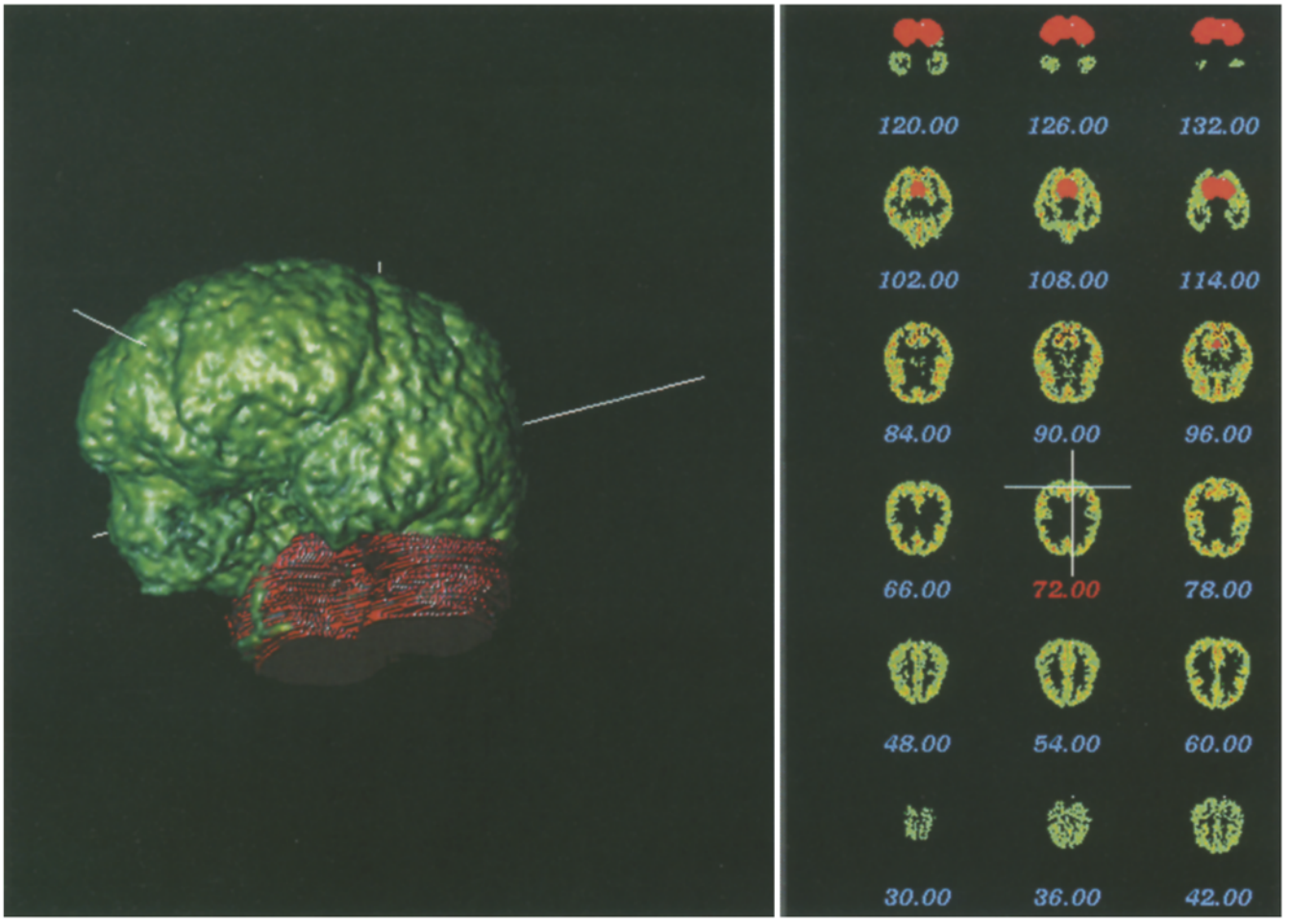

Fig. 7 An oblique view from below the exterior surface of the PET data representing *seeded* BZR binding. The cerebellum data deleted are visualized in *red*. To the right some of the corresponding 2D PET planes are presented. The intersection of the *white lines* indicates the point where the seeding process was initiated

tion. However, the way the data in 3D is presented allows the inspection of the voxel matrix from various angles. This in turn made it possible to visualize the neuroreceptor binding as it was distributed in space and the characterization of the correct 3D topography of the receptor molecule population. Volumes containing high BZR densities were visualized as objects. Using the commercially available computer graphic software, they could be rotated interactively in real time and their forms examined from different angles, giving a strong visual perception of their 3D extension. Not only the distribution of the BZR populations as inspected from the outside of the brain, but also their distribution within the interior of the brain, could be visualized as shown in Figs. 3–6.

These 3D images of the BZR binding in a living human brain represent a new type of physical representation in space of a molecular aspect of the GABA-regulated inhibitory transmitter potential. By use of automated thresholding and seeding techniques, it was also possible to efficiently and automatically define volumes and quantities of the BZR population. The volumes of these structures (generally V_{BZR}) is not identical to the volume of the brain tissue, but represents a new quantifiable measure defined by the presence of BZRs binding to the radioligand and the number of voxels containing such BZRs. The V_{BZR} can be regarded as index of the volume extension of BZR-regulated inhibitory mechanisms in an individual brain or region.

Previous autoradiographic and PET studies of radioligand binding neuroreceptors have supplied values for receptor characteristics such as receptor concentration (B_{max}) and affinity (K_d). Such data have thus far been measured and calculated from a very limited amount of selected ROIs from a few 2D planes through the brain. However, it is obvious that such measures must be regarded as coarse approximations due to, for example, heterogeneous receptor distribution in tissue and partial volume effects in PET studies.

For clinical neuropsychiatric studies the total number of receptors expressed in a gross region, in a specific system or even the whole brain, may be more relevant as a correlate to psychomotor function than a receptor concentration calculated from a few 2D slices through selected parts of the brain (Sedvall et al. 1994). Thus, the development of practical, efficient methods to quantify the *total*

number of receptors (N) or the *volume these receptors take into account* (V_{BZR}^{app}) in the brain or defined regions of it seem pertinent. It should be pointed out that the V_{BZR}^{app} calculated represents an overestimation of the true anatomical volume of BZR tissue due to the limited resolution of the PET camera (Frost et al. 1996). The 3D volume-rendering techniques as showed in the present study offer a significant step in this direction. Thus, the technique applied was also used for the rapid and efficient quantification of the total BZR number in a whole human living cerebrum. The male subject examined by PET in the present study was found to have approximately 18 nmol of BZR binding receptors contained within a voxel matrix of approximately 1.2 L within his cerebrum. Such quantitative neuroreceptor measures from the whole brain or some of its subregions may turn out to be useful individual characteristics for future comparative studies of healthy subjects and patients with neuropsychiatric disorders or vulnerabilities. It does not seem unlikely that this type of measure, representing global values for different aspects of receptor expression, which have not previously been used in clinical neuropsychiatric research, may be related to the specific influence of genes or early external developmental influences. Thus, it may be argued that the response from a brain region is more directly determined by the total receptor number and the spatial extension of these receptors, rather than the receptor density. The total amount of BZRs and the volume they take into account in the brain of an individual human subject as measured in the present study may turn out to be molecular variables as important for biomedical research as other anthropomorphic data such as height, weight, or IQ. In this respect the present methodology and results offer new anthropomorphic dimensions to clinical neuroscience that should be examined with regard to variability within groups of healthy subjects and patients with neuropsychiatric disorders.

In principle, the present methodology should also be useful to visualize and quantify autoradiographic in vitro data from series of consecutive histologic sections through the human brain using neuroreceptor radioligands or other markers (Sedvall and Farde 1995). By such methods a much higher resolution can be obtained than is shown in the present PET approach. It can also be expected that the accelerating availability of specific radioligands for neuroreceptors and their subtypes, as well as other markers, will require more efficient automated procedures to visualize and quantify an increasing number of molecular entities in the human brain. By the combination of in vivo PET and in vitro autoradiography, using appropriate markers, the technology applied and developed in this study offer efficient strategies for rapidly designing computerized information banks for the human brain. Such biochemical data banks in addition to functional information banks (Roland and Zilles 1994) will be indispensable in the search for pathophysiologic mechanisms in neuropsychiatric disorders.

Acknowledgements The radioligand [^{11}C]flumazenil was kindly synthesized by Dr. Christer Halldin. This work was supported by grants from the Swedish Medical Research Council (03560), the National Institute of Mental Health (NIMH), USA (grant no. NH 44814), the Söderström-König Foundation, the Karolinska Institute, and the Swedish Medical Association.

References

Andreasen NC, Oleary DS, Arndt S, Cizadlo T, Hurtig R, Rezai K, Watkins GL, Ponto LLB, Hichwa RD (1995a) Short-term and long-term verbal memory: a positron emission tomography study. Proc Natl Acad Sci USA 92:5111–5115

Andreasen NC, Swayze V, Oleary DS, Nopoulos P, Cizadlo T, Harris G, Arndt S, Flaum M (1995b) Abnormalities in midline attentional circuitry in schizophrenia: evidence from magnetic resonance and positron emission tomography. Eur Neuropsychopharmacol 5:37–41

Argiro VJ (1990) Seeing in volume. Pixel 1:35–39

Bergström M, Boetius J, Eriksson L, Greitz T, Ribbe T, Widén L (1981) Head fixation device for reproducible position alignment in transmission CT and positron emission tomography. J Comput Assist Tomogr 5:136–141

Blomqvist G, Pauli S, Farde L, Eriksson L, Persson A, Halldin C (1990) Maps of receptor binding parameters in the human brain: a kinetic analysis of PET measurements. Eur J Nucl Med 16:257–265

Catmull EA (1974) Subdivision algorithm for computer display of curved surfaces. PhD thesis report UTEC-CSc-74-133, Computer Science Department, University of Utah, Salt Lake City, Utah

Drebin RA, Carpenter L, Hanrahan P (1988) Volume rendering. Comput Graph 22:65–74

Farde L, Hall H, Ehrin E, Sedvall G (1986) Quantitative analysis of D2 dopamine receptor binding in the living human brain by PET. Science 231:258–261

Fiez JA, Raichle ME, Balota DA, Tallal P, Petersen SE (1996) PET activation of posterior temporal regions during auditory word presentation and verb generation. Cereb Cortex 6:1–10

Foley JD, Dam A van, Feiner SK, Hughes JF (1990) The Phong lighting model. In: Computer graphics: principles and practice, 2nd edn. Addison-Wesley, London, pp 729–731

Friston KJ, Frith CD, Liddle PF, Frackoviack RSJ (1991) Comparing functional (PET) images: the assessment of significant change. J Cereb Blood Flow Metab 11:690–699

Frost J, Meltzer C, Zubieta J, Links J, Brakeman P, Stumpf M, Kruger M (1996) MR-based correction of partial volume effects in brain PET imaging. In: Myers R, Cunningham V, Bailey D, Jones T (eds) Quantification of brain function using PET. Academic Press, New York, pp 152–157

Hall H, Litton J-E, Halldin C, Kopp J, Sedvall G (1992) Studies on the binding of [3H]flumazenil and [3H]sarmazenil in post mortem human brain. Hum Psychopharmacol 7:367–377

Hall H, Sedvall G, Magnusson O, Kopp J, Halldin C, Farde L (1994) Distribution of D1- and D2-dopamine receptors, and dopamine and its metabolites in the human brain. Neuropsychopharmacology 11(4):245–256

Halldin C, Stone-Elander S, Thorell J-O, Persson A, Sedvall G (1988) 11C-labeling of Ro 15-1788 in two different positions, and also 11C-labeling of its main metabolite Ro 15-3890, for PET studies of benzodiazepine receptors. Appl Radiat Isot 39:993–997

Harris LD, Robb RA, Yuen TS, Ritman EL (1978) Non-invasive numerical dissection and display of anatomic structure using computerized X-ray tomography. Proc SPIE 152:10–18

Herman GT, Liu HK (1979) Three-dimensional display of organs from computed tomograms. Comput Graph Image Process 9(1):1–21

Kuhar MJ, Lloyd DG, Appel N, Loats HL (1991) Imaging receptors by computer-assisted approaches. J Chem Neuroanat 4:319–327

Lammertsma A, Lassen N, Prevett M et al. (1993) Quantification of benzodiazepin receptors in vivo using 11C-flumazenil: application of the steady-state principle. In: Uemura K, Lassen NA, Jones T, Kanno I (eds) Quantification of brain function. Excerpta Medica, Amsterdam, pp 303–311

Lassen NA (1992) Neuroreceptor quantitation in vivo by the steady-state principle using constant infusion or bolus injection of radioactive tracers. J Cereb Blood Flow Metab 12:709–716

Lassen NA, Bartenstein PA, Lammertsma AA, Prevett MC, Turton DR, Luthra SK, Osman S, Bloomfield PM, Jones T, Patsalos PN et al. (1995) Benzodiazepine receptor quantification in vivo in humans using [11C]flumazenil and PET: application of the steady-state principle. J Cereb Blood Flow Metab 15(1):152–165

Latchaw R E, Ugurbil K, Hu X (1995) Functional MR imaging of perceptual and cognitive functions. Neuroimaging Clin North Am 5:193–205

Levoy M (1988) Display of surfaces from volume data. IEEE Comput Graph Applications 8:29–37

Lorenson WE, Harvey CC (1987) Marching cubes: a high-resolution 3-D surface construction algorithm. Comput Graph ACM SIGGRAPH '87 Conference Proceedings

Mazière M, Hantraye P, Prenant C, Sastre J, Comar D (1984) Synthesis of ethyl 8-fluoro-5,6-dihydro-5-[11C]methyl-6-oxo-4H-imidazo[1,5-a][1, 4]benzodiazepine-3-carboxylate (RO15.1788-11C): a specific radioligand for the in vivo study of central benzodiazepine receptors by positron emission tomography. Int J Appl Radiat Isot 35:973–978

Persson A, Ehrin E, Farde L, Litton J-E, Mindus P, Sedvall G (1985) Imaging of 11-C-labeled Ro 15-1788 binding to benzodiazepine receptors in the human brain by positron emission tomography. J Psychiatr Res 19:609–622

Persson A, Pauli S, Halldin C, Stone-Elander S, Farde L, Sjögren I, Sedvall G (1989) Saturation analysis of specific 11C Ro 15-1788 binding in the human neocortex using positron emission tomography. Hum Psychopharmacol 4:21–31

Price JC, Mayberg HS, Dannals RF, Wilson AA, Ravert HT, Sadzot B, Rattner Z, Kimball A, Feldman MA, Frost JJ (1993) Measurement of benzodiazepine receptor number and affinity in humans using tracer kinetic modeling, positron emission tomography, and [11C]flumazenil. J Cereb Blood Flow Metab 13(4):656–667

Raichle ME (1994) Images of the mind: studies with modern imaging techniques. Annu Rev Psychol 45:333–356

Roland PE, Zilles K (1994) Brain atlases: a new research tool. Trends Neurosci 17:458–467

Russ JC (1995) The image processing handbook, 2nd edn. CRC Press, Boca Raton, Florida

Sedvall G, Farde L, Persson A, Wiesel F-A (1986) Imaging of neurotransmitter receptors in the living human brain. Arch Gen Psychiatry 43:995–1005

Sedvall G, Karlsson P, Lundin A, Anvret M, Suhara T, Halldin C, Farde L (1994) Dopamine D1 receptor number: a sensitive PET marker for early brain degeneration in Huntington's disease. Eur Arch Psychiatry Clin Neurosci 243:249–255

Sedvall G, Farde L (1995) Dopamine receptors in schizophrenia. Lancet 346:743–749

Sokoloff L, Reivich M, Kennedy C, Des Rosiers MH, Patlak CS, Pettigrew KD, Sakurada O, Shinohara M (1977) The [14C]deoxyglucose method for the measurement of local cerebral glucose utilization: theory, procedure, and normal values in the conscious and anesthetized albino rat. J Neurochem 28:897–916

Toga AW (1990) Three-dimensional neuroimaging. Raven Press, New York

Van Zandt WL, Argiro VJ (1989) A new inlook on life. UNIX Rev 7:52–57

Wagner HNJ, Burns HD, Dannals RF, Wong DF, Långström B, Duelfer T, Frost JJ, Ravert HT, Links JM, Rosenbloom SB, Lukas SE, Kramer AV, Kuhar MJ (1983) Imaging dopamine receptors in the human brain by positron tomography. Science 221:1264–1266

Watt A (1991) Volume rendering. In: 3D Computer graphics. Addison-Wesley, London, pp 313–319

Weinhard K, Dahlbom M, Eriksson L, Michel C, Bruckbauer T (1994) The ECAT EXACT HR: performance of a new high-resolution positron scanner. J Comput Assist Tomogr 18:110–118

Wilhems J, Van Gelder A (1991) A coherent projection approach for direct volume rendering. Comput Graph 25:275–284